Fabrication and photoluminescence characteristics of In_2O_3 nanohillocks*

Wei He-Lin(魏合林)†, Zhang Lei(张 磊), Liu Zu-Li(刘祖黎), and Yao Kai-Lun(姚凯伦)

Department of Physics, Huazhong University of Science and Technology, Wuhan 430074, *China*

(Received 27 July 2010; revised manuscript received 29 June 2011)

Uniformly distributed polycrystalline indium nanohillocks are synthesized on silicon substrates with Au catalyst by using the radio frequency magnetic sputtering technique. The results show that the Au catalyst plays a key role in the formation of indium nanohillocks. After thermally oxidizing the indium nanohillocks at 500 °C in air for 5 h, the indium nanohillocks totally transform into In_2O_3 nanohillocks. The energy-dispersive X-ray spectroscopy result indicates that many oxygen vacancies and oxygen–indium vacancy pairs exist in the In_2O_3 nanohillocks. Photoluminescence spectra under an Ne laser excitation at 280 nm show broad emissions at 420 nm and 470 nm with a shoulder at 450 nm related to oxygen vacancies and oxygen–indium vacancies at room temperature.

Keywords: In_2O_3 nanohillocks, magnetron sputtering, growth models, low-dimensional alloy surface

PACS: 81.15.cd, 68.55.–J, 78.55.–m **DOI:** 10.1088/1674-1056/20/11/118102

1. Introduction

In recent years, lower-dimensional (LD) semiconductor nanostructures, such as nanowires, nanorods and nanobelts of several binary oxide systems, including ZnO, SnO_2, In_2O_3, GeO_2,[1−9] have been intensively investigated because of their novel properties (optical, electrical, and magnetic properties) and their potential applications in nano-devices. Among them, the In_2O_3, which is a wide band gap transparent semiconductor material, has been widely used in the microelectronic applications including window heaters, solar cells, and liquid-crystal displays.[10−12] The In_2O_3 nanowires and nanobelts have been prepared by various methods, such as oxidation of indium metal embedded by electrodeposition in anodic alumina membranes,[13] thermal evaporation of indium source materials,[4,5,7] plasma-assisted In_2O_3 nanowires growth with Au film as catalyst,[6] and thermal evaporation of indium oxide source materials.[8]

In this work, uniformly distributed indium nanohillocks and In_2O_3 nanohillocks are fabricated with Au as catalyst by radio frequency (RF) magnetic sputtering technique. First, the indium nanohillocks are grown on silicon wafer with Au catalyst at room temperature and then the indium nanohillocks are thermally oxidized at 500 °C in air. The morphologies and microstructures of the indium nanohillocks and the In_2O_3 nanohillock are characterized by scanning electron microscopy (SEM), transmission electron microscopy (TEM) and X-ray diffraction (XRD).

2. Experimental method

The experiment process could be divided into two steps: indium film deposition process at room temperature and thermal oxidation process. In the first step, the indium films were deposited on silicon substrates without and with Au catalyst by RF magnetic sputtering at room temperature. The magnetron sputtering deposition chamber was maintained at a base pressure of 1×10^{-2} Pa and a working pressure of 333 Pa through mechanical vacuum pump and turbo pump. The sputtering power was kept at 30 W. The Au film was first deposited on the silicon substrate and then the indium film was deposited for all samples. The chamber was filled with 99.999% Ar. The targets were a block of 99.997% indium and a block of 99.999% gold. The targets were all sputter-cleaned in Ar gas for 5 min before deposition. The substrate was an n-type Si (111) wafer with a thin layer of SiO_x. In all cases, the wafer had been cleaned ultrasonically in alcohol and then acetone. The deposition rates for

*Project supported by the National Natural Science Foundation of China (Grant No. 10574047) and the Key Program of the National Natural Science Foundation of China (Grant No. 20490210).

†Corresponding author. E-mail: hlwei@mail.hust.edu.cn

© 2011 Chinese Physical Society and IOP Publishing Ltd

indium and Au were about 3.5 nm/s and 2 nm/s, respectively. The deposition rates were estimated based on the film thickness measured by the SEM. It should be mentioned that the deposition rate in this work is larger than that in our previous work by using direction current (DC) magnetic sputtering method.[14]

Then, the indium film samples were thermally oxidized at 500 °C in air for 5 h. It is well known that the bulk indium crystal hardly reacts with oxygen at room temperature. However, indium reacts with oxygen more easily if the temperature exceeds the melting point of indium. During thermal oxidation at low temperatures ($T < 300$ °C), our experimental results showed that a thin layer of In_2O_3 covered the surface of the indium film. However, the deep layer of the indium film was still hard to react with oxygen. Therefore, a higher temperature (500 °C) was chosen as the thermal oxidation temperature.

The crystal structures of the indium films and its oxidation products were identified by XRD with Cu Kα radiation. The morphologies and the compositions of the products were examined by SEM (FE-SEM, FEI, Sirion 200) equipped with an Energy Dispersive X-ray Detector (EDX). The microstructures of the products were investigated by TEM (FEI, Tecnai G2 20). The photoluminescence (PL) measurement was performed by PL spectra (LS55, Perkinelmer) at room temperature. The excitation source was an Ne laser beam at 280 nm.

3. Results and discussion

Firstly, the pure indium film deposited on silicon substrate without Au catalyst was investigated. The deposition time of indium film was 40 s. The SEM image for pure indium film is shown in Fig. 1. Obviously, the surface of the film is uniform. A few nanohillocks each with a diameter of tens nanometers can be clearly seen from the film surface. By investigating the morphology evolvement with deposition time (not shown here), we find that the size of hillocks increases with deposition time increasing. This phenomenon was described in our previous work by direct current (DC) magnetron sputtering method.[15,16] It was suggested that these nanohillocks were formed by the compressive stress in the indium film generated in the grain coalescence process. It is interesting to note that many nanodots (white dots in Fig. 1) appear on the film surface. We speculate that the drive force of the nanodot growth comes from the compressive stress in indium grains (or nanohillocks).

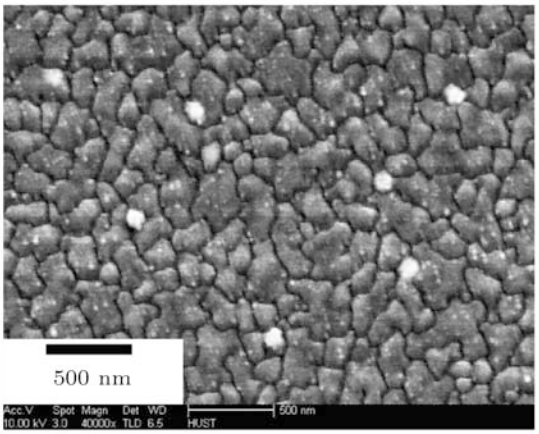


Fig. 1. SEM image for pure indium film without Au catalyst.

Then, the indium film was deposited on silicon substrate with Au catalyst by RF magnetic sputtering. The Au film was first deposited on the silicon substrate and then the indium film was deposited. The deposition times of the Au catalyst and indium were 5 s and 40 s, respectively. The thickness of the Au catalyst was about 10 nm. The morphology of the indium film is shown in Fig. 2. The SEM image clearly shows that a large number of isolation indium nanohillocks form on film surface. The sizes of the nanohillocks are significantly different. The average size of the nanohillocks is about 100 nm. The spacing between two nanohillocks is about 50 nm and the density of the nanohillocks is about 6.0×10^9 cm^{-2}. Comparing Fig. 2 with Fig. 1, it is obvious that two morphologies are quite different. Without Au catalyst, the nanohillocks grow from the condensed indium film and the indium film has a maze structure. However, with Au catalyst, the isolation indium nanohillock stands on the film surface. Obviously, the formation mechanism of the indium nanohillocks with Au catalyst in Fig. 2 is different from that in Fig. 1. This result implies that the Au catalyst plays a key role in the formation of the isolation indium nanohillocks. Figure 2(b) is the magnified image of Fig. 2(a). We note that there are still many nanodots on the surfaces of the nanohillocks. The size of the nanodots is about 50 nm. Comparing the present result with our previous result,[14–17] two type magnetron sputtering methods (RF and DC) present quite different nanohillock morphologies (the inset in Fig. 2(a) shows the In nanorods fabricated by DC magnetron sputtering method). The reason for this is not clear now.

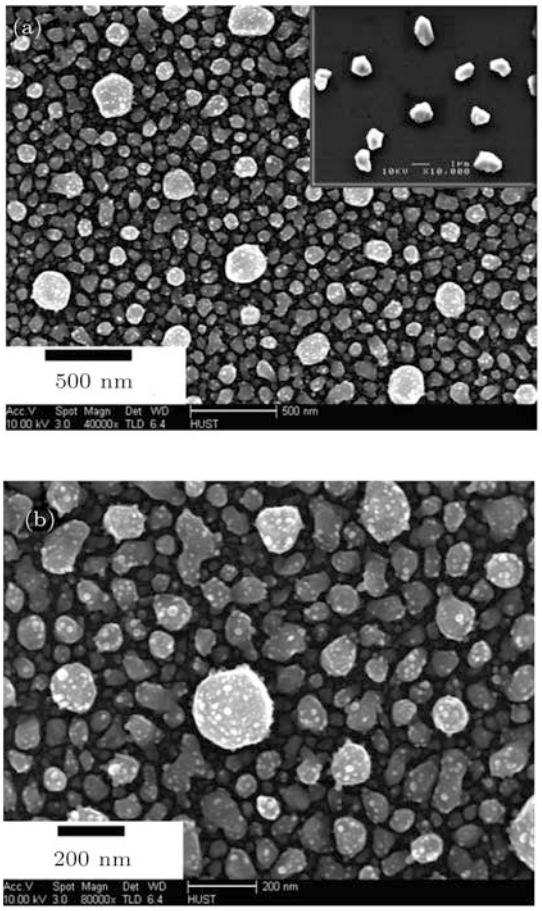


Fig. 2. (a) SEM image for indium nanohillock with Au catalyst by RF magnetron sputtering method, with the inset showing the In nanohillocks fabricated by DC magnetron sputtering method; (b) magnified image of indium nanohillocks.

Several materials (such as glass and carbon film) were also tested as substrates. We found that the nanohillock formation was independent of the substrate material. Therefore, a sample was prepared by depositing first Au and then indium on carbon film coated on a copper grid for TEM investigation. The deposition times of the Au film and the indium film were 5 s and 40 s, respectively. The TEM image of the indium film is shown in Fig. 3. Several nanohillocks (dark area) can be clearly seen from the image in Fig. 3(a). Their average size is about 100 nm. The image in Fig. 3(b) is plane-view high resolution transmission electron mircoscopy (HRTEM) image of one indium nanohillock (marked with B in image of Fig. 3(a)). The separation between the lattice fringes is 0.320 nm, which is in good agreement with the lattice plane spacing d (010) of body-centred tetragonal (BCT) indium lattice with lattice parameters $a = b = 0.323$ nm and $c = 0.495$ nm.

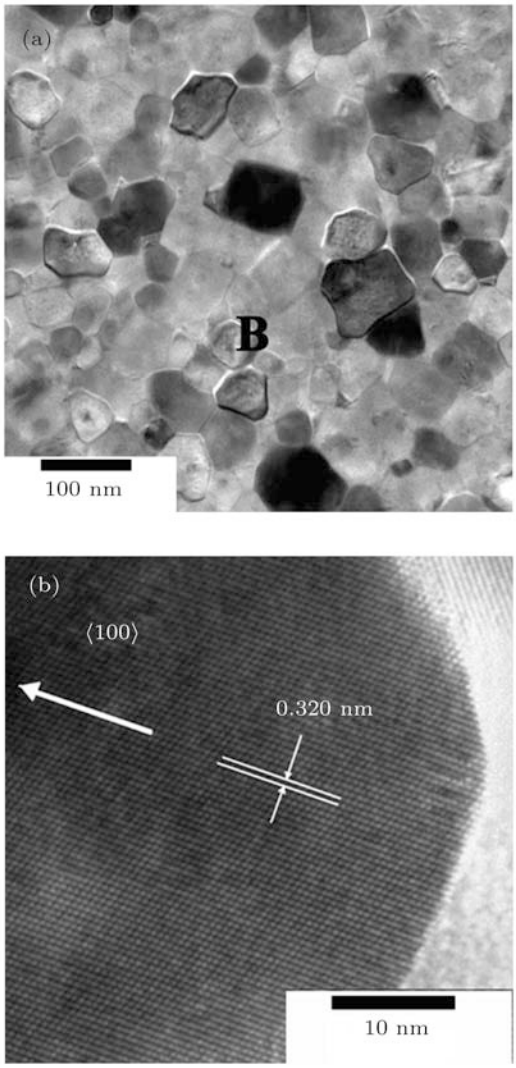


Fig. 3. TEM images of indium nanohillocks with Au catalyst: panel (a) shows the bright-field image and panel (b) displays the HRTEM side-view image of a nanohillock.

Figure 4(a) shows a typical XRD pattern of the pure indium film without Au catalyst on the silicon substrate. The XRD result indicates that the crystalline structure of the deposition film is BCT indium. According to the PDF data No. 85-1409, we note that the relative intensities of the diffraction peaks in Fig. 4(a) are different from those of the powder diffraction peaks, especially for (101) peak. This result implies that (101) texture exists in pure indium film. The XRD pattern of the indium films with Au catalyst is shown in Fig. 4(b). The XRD pattern in Fig. 4(b) is totally different from that in Fig. 4(a). The indium film with Au catalyst has a strong (110) texture. The (101) peak (strong in Fig. 4(a)) becomes weak in Fig. 4(b). Some diffraction peaks ((002), (112), (103) and (211)) disappear. This result indicates that the Au catalyst strongly affects the microstructure (or

texture) of the indium film in the deposition process.

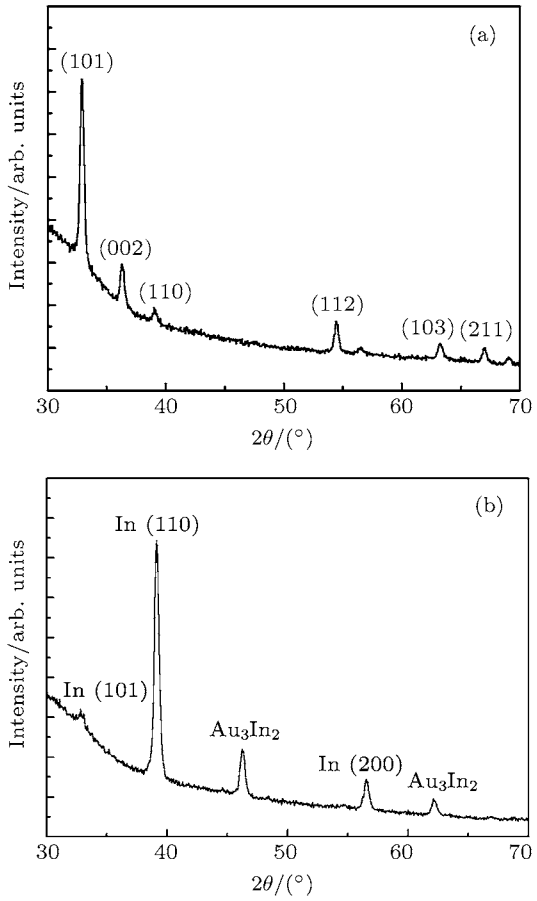


Fig. 4. XRD patterns of the indium films: for pure indium film without Au catalyst (a) and for Indium nanohillocks with Au catalyst (b).

It is worth while to note that there is an Au_3In_2 alloy peak in Fig. 4(b). This peak implies that low-dimensional (LD) Au/In alloy layer forms on the substrate surface in the deposition process. In our earlier reports,[14,17] we found that the LD Au_3In alloy layer plays a chemistry-mediated role in indium nanohillock formation process. This LD Au/In alloy layer modulates the substrate surface from wetting to non-wetting surface. On the LD Au/In alloy surface, the indium atoms, even small clusters, can easily move. After several clusters aggregating, the indium nanohillock grows up. This self-assembled growth mechanism is different from the mechanism in the previous report.[18] The different alloy compositions, Au_3In_2 in this work and Au_3In in our earlier work, may result from the different deposition methods.

After thermally oxidizing the sample (deposition times of Au and indium films were 10 s and 40 s, respectively) at temperature of 500 °C in air for 5 h, the microstructure of the products was investigated by XRD. The XRD pattern is shown in Fig. 5. The diffraction peak can be indexed to In_2O_3 with cubic structure of bixbyite Mn_2O_3 type with the lattice constant $a = 1.012$ nm. There is no BCT indium peak appearing in Fig. 5. This implies that the indium nanohillocks totally transform into In_2O_3 nanohillocks after thermally oxidizing. We note that the structure of the alloy layer changes from Au_3In_2 into $Au_{10}In_3$ after being thermally oxidized. The appearance of the strong Au (200) and Au (111) peaks is because of the longer deposition time of the Au catalyst.

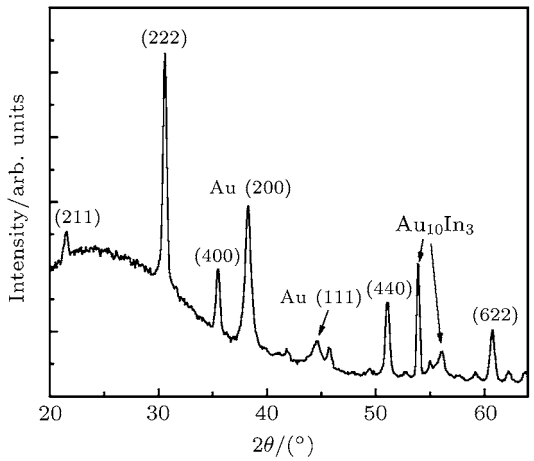


Fig. 5. XRD pattern of the In_2O_3 nanohillocks after thermally oxidizing the indium nanohillock at 500 °C in the air for 5 h.

The SEM images of the In_2O_3 nanohillocks are shown in Fig. 6. The magnified image of the In_2O_3 nanohillocks is shown in Fig. 6(b). The average size of the In_2O_3 nanohillocks is about 150 nm. Obviously, the size of the In_2O_3 nanohillock is larger than that of the indium nanohillocks before being thermally oxidized. The density of the In_2O_3 nanohillocks is about 2.0×10^9 cm^{-2}, which is less than that before being thermally oxidized. The increase of the nanohillock diameter and the decrease of the nanohillock density after being thermally oxidized are because of the diffusion of the indium atom and the coalescence of smaller nanohillocks in the thermal oxidation process, respectively.

The EDX pattern by focusing the electron beam on an In_2O_3 hillock (marked A in Fig. 6(b)) is shown in Fig. 7. After analysing the EDX data, we find that the atomic ratio of indium and oxygen is 44:56. The existence of Si and Au peak reveals that the nanohillocks are deposited on silicon substrate with the Au catalyst. The normal atomic ratio of indium

and oxygen in In_2O_3 should be 2:3. According to the EDX analysis, we can conclude that there exist many oxygen vacancies (or oxygen–indium vacancy pairs) in the In_2O_3 nanohillocks.

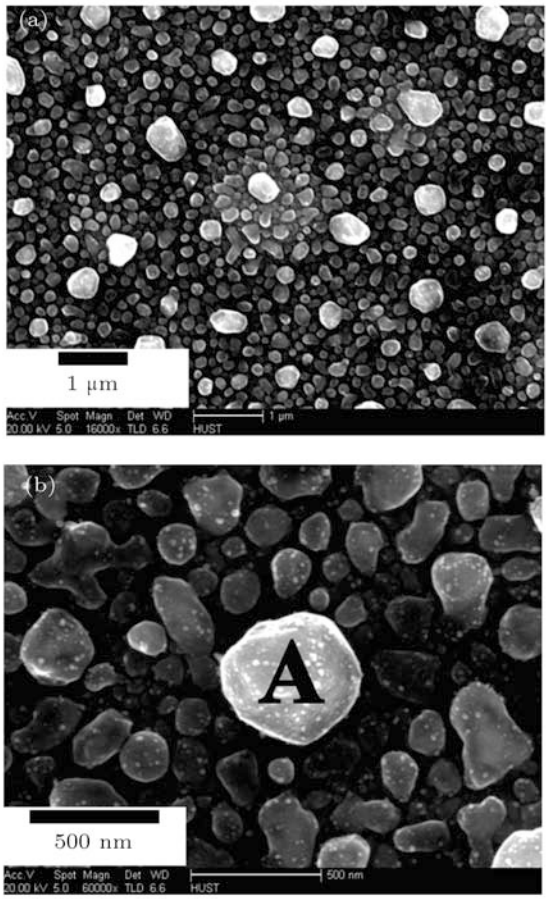


Fig. 6. SEM image of the In_2O_3 nanohillocks synthesized by thermally oxidizing the indium film (a) and magnified image of In_2O_3 nanohillocks (b).

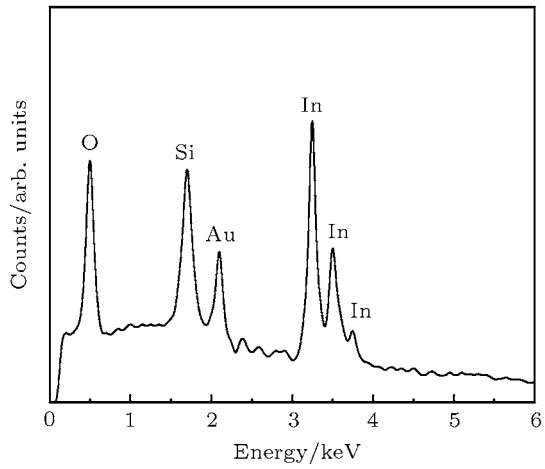


Fig. 7. EDX spectrum of the In_2O_3 nanohillocks.

The PL of the In_2O_3 nanohillocks was studied at room temperature using an Ne laser excitation at 280 nm. The result is shown in Fig. 8. Earlier reports indicated that the bulk In_2O_3 cannot emit light at room temperature.[19] However, indium–oxide thin film exhibited two distinct peaks in the PL spectrum at 415 nm and 440 nm[20] even at 637 nm.[21] From Fig. 8 (curve *a*), we find that for our In_2O_3 nanohillocks the broad PL emission peaks appear at 420 nm and 470 nm with a shoulder at 450 nm under the excitation at 280 nm but no PL emission peak occurs when wavelength is larger than 500 nm. In addition, the PL spectrum of the In_2O_3 film without using Au catalyst by thermally oxidizing the sample (Fig. 1) at temperature of 500 °C in air for 5 h was measured for comparing the PL spectrum of the indium film with using Au catalyst (curve *b* in Fig. 8). We find that there are two small peaks at 417 nm and 438 nm in the PL spectrum. This result is consistent with that of the PL spectrum of indium–oxide thin film in Ref. [21]. In order to obviate the effect of In–Au alloy on the PL emission spectrum of In_2O_3 nanohillocks, a sample with thicknesses of the Au catalyst and In of about 10 nm and 17 nm respectively was fabricated. In this case, there was no nanostructure on the surface except In–Au alloy. The PL spectra show no peak appearing (not shown here). This implies that the PL spectrum (curve *a* in Fig. 8) induced by the In_2O_3 nanohillocks.

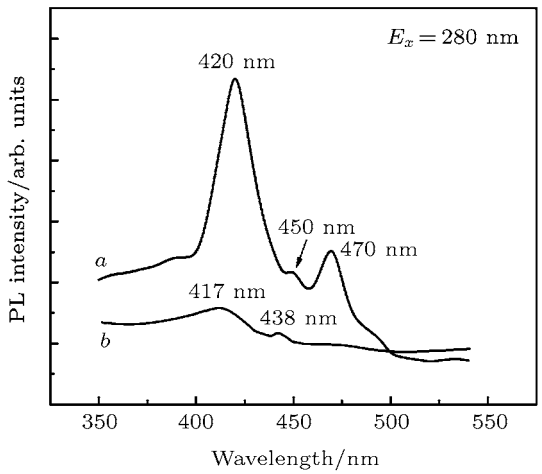


Fig. 8. The PL peaks of the In_2O_3 nanohillocks (curve *a*) and In_2O_3 film (curve *b*) at room temperature using an Ne laser excitation at 280 nm.

The PL spectra of the In_2O_3 nanostructures have been well studied.[4,7,8,22] However, the wavelengths of the emission light are quite different for different nanostructures. Guha *et al.*[4] observed the PL peak at 470 nm from the In_2O_3 nanopyramid and nanocolumn structure. Jeong *et al.*[7] reported a peak at 570 nm from In_2O_3 nanobelt. Wu *et al.*[8] found two peaks at 416 nm and 435 nm from the single crystalline

In_2O_3nanowire. Zhou *et al.*[22] observed PL peaks at 480 nm and 520 nm from the In_2O_3 nanoparticle. These emission peaks commonly refer to the deep level or trap state emissions due to oxygen deficiencies.

In the present case, the In_2O_3 nanostructure is fabricated by thermally oxidizing the indium nanohillock at higher temperature (500 °C). We speculate that this method may induce a higher density of oxygen vacancies and oxygen–indium vacancy pairs in In_2O_3 nanohillock because of partially incomplete oxidation. The EDX result (Fig. 7) confirms this speculation. This implies that in the In_2O_3 nanohillock there exist many singly ionized oxygen vacancies ($V_O^{\bullet}$) and other oxygen vacancies such as $V_O^{\times}$ and $V_O^{\bullet\bullet}$. These oxygen vacancies may lead to the formation of new energy levels in the bandgap. It is therefore reasonable for us to believe that the blue light emission can be attributed to the emission from deeper energy levels induced by oxygen vacancies and indium–oxygen vacancy centres.

During the excitation, the acceptors may be formed by indium–oxygen vacancy centres $(V_{In}, V_O)^{\times}$, and the oxygen vacancies $V_O^{\times}$ and $V_O^{\bullet}$ may act as donors. The excitation process may be written as[8]

$$(V_{In}, V_O)' + V_O^{\bullet} + h\upsilon \rightarrow (V_{In}, V_O)^{\times} + V_O^{\times}.$$

The reverse process of this reaction may produce the broad blue–green PL emission. Luminescence process can be divided into two steps: (i) The indium–oxygen vacancy centre $(V_{In}, V_O)'$ and the oxygen vacancy $V_O^{\bullet}$ may be excited by high energy light and then an electron may transfer from indium–oxygen vacancy centre $(V_{In}, V_O)'$ to oxygen vacancy $V_O^{\bullet}$ to form the accepter $(V_{In}, V_O)^{\times}$ and donor $V_O^{\times}$; (ii) an electron in donor level $V_O^{\times}$ may be captured by a hole on an acceptor $(V_{In}, V_O)^{\times}$ to form a trapped exciton and the trapped exciton is recombined radioactively to produce observed blue–green emission. Several emission peaks may originate from radiative recombination of different vareties of trapped excitons. Of course the PL mechanism of nanohillock needs further investigation.

4. Conclusion

The indium nanohillocks were synthesized on silicon substrates with Au catalyst by using RF magnetic sputtering approach at room temperature. The Au catalyst plays an important role in the formation of the indium nanohillocks. By thermally oxidizing the indium nanohillocks at 500 °C in the air for 5 h, the In_2O_3 nanohillocks were fabricated. The EDX result indicates that there exist a large number of oxygen vacancies and oxygen–indium vacancies in the In_2O_3 nanohillocks. The blue PL peaks at 420 nm and 470 nm are observed at room temperature which is attributed to the existence of a large number of oxygen vacancies in the In_2O_3 nanohillock. The detailed mechanism of the photoluminescence in the In_2O_3 nanohillock needs to be investigated systematically. The In_2O_3 nanohillocks may have potential application in advanced optical devices in the future.

Acknowledgement

The authors are grateful to the Analytical and Testing Centre, Huazhong University of Science and Technology for its support.

References

[1] Xiao S, Su X R, Li C, Han Y B, Fang G J and Wang Q Q 2008 *Chin. Phys.* B **17** 1291
[2] Huang M H, Wu Y, Feick H, Tran N, Weber E and Yang P 2001 *Adv. Mater.* **13** 113
[3] Gu F, Wang S F, Lü M K, Cheng X F, Liu S W, Zhou G J, Xu D and Yuan D R 2004 *J. Cryst. Growth* **26**2 182
[4] Guha P, Kar S and Chaudhuri S 2004 *Appl. Phys. Lett.* **85** 3851
[5] Jia H B, Zhang Y, Chen X H, Shu J, Luo X H, Zhang Z S and Yu D P 2003 *Appl. Phys. Lett.* **82** 4146
[6] Li S Q, Liang Y X and Wang T H 2005 *Appl. Phys. Lett.* 87 143104
[7] Jeong J S, Lee J Y, Lee C J, An S J and Yi G C 2004 *Chem. Phys. Lett.* **384** 246
[8] Wu X C, Hong J M, Han Z J and Tao Y R 2003 *Chem. Phys. Lett.* **373** 28
[9] Bai Z G, Yu D P, Zhang H Z, Ding Y, Wang Y P, Gai X Z, Hang Q L, Xiong G C and Feng S Q 1999 *Chem. Phys. Lett.* **303** 311
[10] Liang C H, Meng G W, Lei Y, Phillipp F and Zhang L D 2001 *Adv. Mater.* **13** 1330
[11] Zheng M J, Zhang L D, Li G H, Zhang X Y and Wang X F 2001 *Appl. Phys. Lett.* **79** 839
[12] Li X, Wanlass M W, Gessert T A, Emery K A and Coutts T J 1989 *Appl. Phys. Lett.* **54** 2674
[13] Chun H J, Choi Y S, Bae S Y and Park J 2005 *Appl. Phys.* A: *Mater. Sci. & Proce.* **81** 539
[14] Wei H L, Zhang L, Liu Z L, Huang H C and Zhang X X 2006 *J. Cryst. Growth* **297** 300
[15] Wei H L, Huang H C and Zhang X X 2006 *Chin. Phys. Lett.* **23** 1627
[16] Wei H L, Zhang X X and Huang H C 2006 *Chin. Phys. Lett.* **23** 1880
[17] Wei H L, Huang H C, Woo C H, Zhang X X and Zhou L G 2004 *Appl. Phys. Lett.* **84** 5401
[18] Moriarty P 2001 *Rep. Prog. Phys.* **64** 297
[19] Ohhata Y, Shinoki F and Yoshida S 1979 *Thin Solid Films* **59** 255
[20] Kaleemulla S, Reddy A S, Uthanna S and Reddy P S 2009 *J. Alloys Compd.* **479** 589
[21] Lee M S, Choi W C, Kim E K, Kim C K and Min S K 1996 *Thin Solid Films* **279** 1
[22] Zhou H J, Cai W P and Zhang L D 1999 *Appl. Phys. Lett.* **75** 495